CEM924 Literature Report

Spatially-Resolved XPS --- Photoemission Electron Microscopy (PEEM)

Submitted by Haihong Jiang

1. Introduction

Effective spatially resolved chemical analysis techniques have been long for the studies in material, environmental and biological sciences. XPS, NMR and IR are known as having excellent chemical speciation but not spatially sensitive, whereas SEM, TEM are characterized as having high spatial resolution but inadequate capability for chemical identification. For the last 20 years enormous efforts have been made in many laboratories to develop surface analysis techniques combining spectroscopic chemical information with high spatial resolution. However, there are several serious drawbacks should be overcome, such as radiation damage, low signal-to-background and signal-to-noise ratios, and poor sensitivity to different chemical states of a given element. These problems can be solved to a large extent by using photoemission electron microscopy (PEEM). Since 1990's significant progresses have been made in this technique, particularly due to the construction of dedicated synchrotron radiation sources which provide a high photon flux in the UV and soft X-ray ranges. X-ray illumination from a synchrotron source can be monochromatized and continuously varied in energy, which allows the X-PEEM to additionally acquire chemical information. The tunability and polarization of synchrotron light also allows near-edge photo absorption experiments (NEXAFS/XANES) to be performed by measuring the total electron yield as a function of photo energy, with a lateral resolution reaching 20 nm [1]. In addition, photoelectron spectra can be measured near the threshold, where the photoionization cross-section is highest, or 40-100 eV above where the surface sensitivity is highest. At last, the energy resolution can be sufficiently high that elemental and even chemical state mapping is possible and X-PEEM images may contain additional contrast, depending on photon energy, due to X-ray absorption by localized elements in a specific chemical state. All

these make X-PEEM to be an extremely flexible and widely used analytical tool for the study of a wide range of materials [2,3].

2. X-PEEM principles

2.1. Basic concepts in spatially localized imaging detection

Spatial localization can be achieved by allowing a certain area of the sample to be exposed to the soft X-ray source to collect signal (i.e. emitted electrons) from a small region of the sample. The spatial localization is occurring on the detection side of the technique. Theoretically, this requires an appropriate lens system to collect as much emission as possible from the desired part of the surface and focus it onto a detector as illustrated in a schematic fashion below (Fig.1).

Error! Unknown switch argument.

Fig. 1. Principles of spatial-resolved imaging

In order to get an image of the surface using a single detector it is necessary to either scan the sample position underneath the detection system or make use of additional scanning plates in the electron-optical focusing system.

Spatial resolution r, is determined by the projection of the cyclotron radius of the photoelectrons in a plane perpendicular to the field at the sample. This is given by

$$r = \frac{\sqrt{2mE}}{eB_{sam}} \sin\theta$$

where E is the electron kinetic energy; B_{sam} is the field strengths at the sample; is the angle between the magnetic field axis and the electron trajectory (G.D. Waddill, 1991).

2.2. Principles of X-ray photoemission electron microscopy (X-PEEM)

The basic idea in a PEEM is to illuminate an area on the sample and then pass the ejected photoelectrons through an electron microscope column, thus producing an enlarged image of the illuminated spot on the sample surface. Fig.2 and Fig. 3 are principle schemes of X-PEEM installed in the Synchrotron Radiation Center of the University of Wisconsin-Madison and Advanced Light Source of Lawrence Berkeley

National Laboratory separately. In spite of some slight instrumental differences, they share the same basic structure and principles [4].

Error! Unknown switch argument.

Error!Error! Unknown switch argument.

Fig. 2. Scheme of the MEPHISTO X-PEEM in SRC of the UW-Madison

Fig. 3. Scheme of X-PEEM (PEEM2) in ALS

X-PEEM is a full field imaging technique based on the illumination of the sample with tunable synchrotron X-rays that have very high brightness and makes it possible to obtain a sufficient signal at a high spatial resolution. Monochromatize X-rays from a synchrotron source excite photoemission (mainly low energy secondary electrons) from the sample surface. The emitted photoelectrons are accelerated towards the microscope by a strong electric field between the sample and the first electrode of the electron optical system (Objective Lens) and then pass through Intermediate Lens and Projective Lens, finally a magnified image is formed on the detector (Chevron style multichannel plate and phosphor screen) that converts electrons into visible light, which is detected by a CCD camera [5,6]. The microscopic aperture in the back focal plane of the objective lens benefits spatial resolution by rejecting all but a narrow band of photoelectron kinetic energies and hence reducing chromatic aberration. Because the detected particles are electrons instead of photons, the experiment must be done in ultrahigh vacuum, this precludes the investigation of wet samples.

2.3. Contrast mechanisms of X-PEEM

There are various contrast mechanisms available in X-PEEM (as shown in Fig. 4).

Fig. 4. Contrast mechanisms in X-PEEM

X-PEEM can show topographical contrast due to the application of the strong electric field between the sample and the first lens. Local topographical features distort

Error! Unknown switch argument.

Error! Unknown switch argument.

Fig. 5. X-PEEM image of Pd stripes on Si

Fig. 6. SEM image of Pd stripes on Si

the field, which results in distortions of the electron trajectories, and therefore, contrast in the image. Fig. 5 and 6 are X-PEEM and SEM images of Pd stripes on Si respectively. For comparison, Pd stripes on Si are imaged using X-PEEM and SEM. The observed contrast is dominated by lateral variations of the work function. Thus PEEM is surface sensitive and reveals details of the topography with 3D effects on the Pd stripes, which are not observed in SEM.

Error! Unknown switch argument.

Fig. 7. X-PEEM image of element distributions

Elemental contrast is achieved by tuning the incident x-ray wavelength through absorption edges of elements [7,8]. The resulting photoelectron emission intensity is strongly enhanced at absorption edges. Areas on the surface containing the corresponding element emit more photoelectrons and thus appear bright in the X-PEEM image at a given absorption edge X-ray energy. Fig.7. Shown opposite are the distributions of iron, chromium, vanadium and manganese in a spray-coated resistant layer of metal nitrides prepared and studied by the Swiss Institute of Standards (EMPA). The black bar is 50 hm. The arrows point out particles containing only one type metal, giving an idea of the range of particle sizes present in the coating.

Error! Unknown switch argument.

Fig. 8. X-PEEM spectroscopy of chemical contrast in different compounds

The photon energy threshold at which the radiation is sufficiently energetic to eject electrons from the sample may shift in different compounds. This chemical shift depends on the oxidation state. Near Edge X-ray Absorption Fine Structure (NEXAFS) spectroscopy can be applied to obtain the information on the chemical state of an

element. The fine structure represents transitions between the core level and unoccupied levels below threshold. XANES spectroscopy can be a probe of unoccupied states in atoms, molecules or crystals [9]. The spectra opposite in Fig.8.shows the absorption structures in the fingerprint region at the L-edge in a range of sulfur-oxygen compounds. Each peak represents a transition from a core level to an unoccupied antibonding orbital formed when the sulfur and oxygen atoms bond covalently according to Molecular Orbital Theory.

Magnetic domain contrast can be achieved from magnetic circular dichroism (XMCD) or magnetic linear dichroism (XMLD) by using polarized synchrotron radiation. XMCD spectroscopy can determine the size, the directions, and the anisotropies of the atomic magnetic moments. In a magnetic metal the *d* shell has a spin moment that is given by the imbalance of spin-up and spin-down states with different occupation. Absorption of right circularly polarized light mainly excites spin-up photoelectrons. Since spin flips are forbidden in electric dipole transitions controlling X-ray absorption and the empty state must have same spin as the emitted electron, the

Fig. 9. Images and local spectra from a ferromagnetic cobalt layer on an antiferromagnetic $LaFeO_3$ substrate

measured resonance intensity is a function of the number of empty *d* band states of the certain spin. XMLD can be utilized to study the properties of antiferromagnetic materials. Because of the lattice symmetry of the molecular the charge distribution around the atoms is nearly spherical and no liner dichroism effect exists in the absence of magnetic interactions [10,11]. The alignment of the local atomic spins along this axis breaks the symmetry of the charge through the spin-orbit coupling. As a result the charge shows an ellipse-like distortion about the magnetic direction in the unit cell. This charge anisotropy results in an asymmetry of the absorption of linearly polarized X-rays. Antiferromagnetic contrast shown in Fig.9. (a) is obtained at the Fe L-edge using linear dichroism (XMLD). (b) Ferromagnetic contrast is obtained at the Co L-edge using circular dichroism

(XMCD) [21]. The arrows indicate the in-plane orientation of the antiferromagnetic axis and ferromagnetic spins. It can be seen that the ferromagnetic Co domains align with the substrate antiferromagnetic domains, but can split into subdomains with opposite magnetization. Spatial resolution of these two images is 20 nm.

3. Instrumental description of X-PEEM

3.1. X-PEEM specifications

Fig. 10 shows the optic layout of a X-PEEM. Fig. 11 and Fig. 12 are the appearance of X-PEEM apparatus manufactured by the OMICRON Company and Advanced Light Source respectively. The tunable synchrotron X-ray beam is focused on the sample with a spot size of 30 ×30 μm. The objective lens is of conical shape allowing the sample to be illuminated by the x-ray beam at a 30° angle. The photo-emitted electrons are accelerated by the immersion objective lens and generate an intermediate image with a magnification of m=10. In order to reduce spherical and chromatic aberrations the microscope is designed for a rather high accelerating voltage of 30 kV. Three corrector elements are incorporate into the microscope column to accommodate for lens imperfections and misalignment of the individual components. An octopole stigmator is located in the back focal plane of the objective lens for the astigmatism correction. There are two hexapole deflectors, one installed behind the stigmator, the other at the back focal plane of the intermediate lens, to correct the beam deflection caused by misalignment of the lens elements. An angle-limiting aperture is also located in the back plane of the objective lens. It has an electron energy filtering effect and therefore reduces the chromatic aberrations. Because the stigmator/deflector arrangement does not leave enough space, a transfer lens with a magnification of unity is added to form another (conjugate) back focal plane for the aperture. The intermediate and projective lens form an enlarged image on a phosphorous screen, and then the image is transferred to a slow-scan CCD camera using a fiber-optics coupling with a 1:2 taper. The calculated spatial resolution is about 20 nm for this design. The heating limit of a sample is up to 1000 °C. Sample

preparation chamber equipped with sputter gun, evaporators, heating, quartz crystal thickness monitor, and magnetic fields up to 800 Oe. XMCD, XMLD, and NEXAFS chamber for reference spectra are in alternating magnetic fields up to 750 Oe [12].

Fig. 10. Instrumental layout of the X-PEEM

Error! Unknown switch argument.

Fig. 11. *OMICRON* FOCUS IS-PEEM

Fig. 12. *ALS* PEEM2

3.2. Beamline characteristics of X-PEEM

Error! Unknown switch argument.

Fig. 13. Schematic layout of X-PEEM Beamline 7.3.1.1. at the ALS.

Fig.13. shows the schematic layout of X-PEEM Beamline 7.3.1.1. installed by the ALS, and Table 1 is its main specification data.

Table 1. Main specification data of Beamline 7.3.1.1. at ALS

Photon Energy Range (eV)	**Photon Flux (photons/s/0.1%BW)**	**Spectral resolution (E/_E)**	**Polarization**	**Spatial Resolution (nm)**	**Samples**
170-1500	$3x10^{12}$	1800	Linear or circular	20 (NEXAFS) 50 (XMCD)	UHV-Compatible solids (up to $1cm^2$ in area)

The use of bend magnet gives the choice of linearly or circularly polarized radiation. Circularly polarized radiation is obtainable by means of a movable aperture that selects

light from above or below the horizontal plane. The spherical grating monochromator is entrance slitless and delivers monochromatic radiation in the energy range of 170-1500 eV with a resolving power of E/ E = 1800 and 3×10^{12} photons/s/0.1%BW at 800eV. The sample is placed in the monochromatic focal plane, without the use of exit slits as typical for conventional systems. This results in an energy dispersed vertical line. Over the typical field of view however of 30 mm the wavelength is essentially fixed. The X-ray beam is focused on the sample with a spot size of 30×30 hm. X-PEEM at Beamline 7.3.1.1. is equipped with a surface science preparation chamber and load-lock system for fast sample transfers, as well as an electron beam evaporator for deposition. The combination of X-ray spectroscopy and high spatial resolution photoemission electron microscopy together with sample preparation capabilities make the X-PEEM a very versatile instrument in surface and materials science.

4. Application examples of X-PEEM

Major applications of X-PEEM include achieving surface or interface imaging at high resolution [13], semiconductor wafer analysis and chemical control by using chemical imaging and video speed imaging [6,14,15], imaging spectroscopy micro-patterned thin films of complex materials [8], superconductor characterization and control of device function, magnetic domain imaging of magnetic recording materials, elemental and chemical bonding contrast imaging of hard disk coatings and sliders [4,16], dewetting and decomposition phenomena of thin polymer blends and bilayers, *in-situ* observation of catalytic reactions [17, 18], and had extended to the area of biology and medicine [19].

4.1. Pt/Co/Pt multilayers on Si

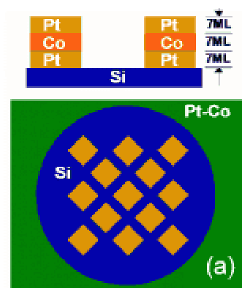

Fig.14. X-PEEM imaging and spectra analysis of Pt/Co/Pt multilayers on Si

Fig.14. Left part shows the image of etched Pt/Co/Pt multilayers (area (b)) on the substrate (area (c)) of Si. Area (a) is the untreated area close to the circular Si substrate containing only Pt/Co. The image was taken at an excitation energy of 95 eV using the synchrotron radiation. The middle picture of Fig.14. is the schematic diagram of the examined surface in section (top) and plan (bottom). Fig.14. Right part shows the spectroscopy of selected areas on the image demonstrates different chemical composition of untreated (a) and etched (b) Pt/Co surface [20]. The spectra of area (b) and (c) both show a sharp peak at 25 eV bonding energy indicating the presence of Si substrate, originates form the 2s state of oxygen in SiO_2, whereas this Si peak did not appear at the spectra of area (a) which only shows the peak of Pt-Co layer. The work function difference between Pt/Co multilayers (b) and Si substrate (c) only 100 meV, and the work function of the closed Pt-Co area (a) is 2 eV higher than them. All these indicate that etched Pt/Co multilayers have undergone alloying with the Si substrate, but the closed Pt-Co area remained unchanged.

4.2. Semiconductor structures of multicrystalline silicon

Fig. 15 and 16 present a new experiment for photoemission electron microscopy by the use of undulator radiation, which has been set up at the beamline U2 at the Berlin electron storage ring BESSY-I. A mobile UHV –chamber was built to combine spectro-microscopy via PEEM with conventional XPS using an additional hemispherical XPS analyzer.

Error! Unknown switch argument.

Fig. 15. Experimental set-up at the direct port of the undulator beamline U2 at BESSY-I.

Error! Unknown switch argument.

Fig. 16. UHV-device consisting of the PEEM with μESCA and a hemispherical XPS-analyzer.

By using this technique, a lot of research investigations have been done on grains and grain boundaries on multicrystalline silicon without removing the native oxide, and the various precipitations seen in the PEEM were studied using μNEXAFS [14]. The mapping of precipitates in multicrystalline silicon, as shown in Fig. 17, indicates that there are significant differences at the Ca-2p and K-2p threshold which are observed around the bright spot in field 1, but not observed on the grain boundaries in field 2. Then it can be

Error! Unknown switch argument. **Error! Unknown switch argument.**

Fig.17. μNEXAFS-spectra of multicrystalline silicon. The spectra where taken on a light sample section (field 1) and on grain boundaries (field 2) of the PEEM-image shown on the top right.

Fig. 18. The PEEM-Image of accumulation of Na on the multicrystalline silicon.

concluded that there is no Ca and K on top of the Si native oxide because Ca or K on top of the oxide would exist as a Ca-oxide and K-oxide and should enhance the O-1s contribution in that area significantly. So the Ca and K contamination must be exist below or within the Si native oxide.

Fig.18. is the images of an accumulation of sodium on the surface of mc- Si. The left PEEM image was taken after transferring the sample. After 12 h under vacuum (UHV) the image of the same sample section on the right-hand side was taken, and there are no more mc-Si structures in this image, only some very bright spots. An obvious difference is visible at the emission at 45.7 eV kinetic energy which belongs to Na-2p. This is supported by the secondary electron onset: the light circular shows a workfunction of 2.8 eV whereas the dark part has a workfunction of 5.0 eV.

5. Summary

The wide range of contrast mechanisms combined with the surface sensitivity and high spatial resolution make X-PEEM a very useful tool for the study of surface science. It is characterized by:

- Full field, real time imaging technique.
- High spatial resolution (2~20 nm) energy filtering of complete images at any magnification and at video rate.
- Can acquire elemental and chemical information as well as topographic imaging.
- Suitable for near-edge x-ray absorption fine-structure spectroscopy (NEXAFS) and x-ray magnetic circular dichroism (XMCD) and x-ray magnetic linear dichroism (XMLD) spectroscopy of microscopic areas on sample surfaces and for imaging.
- The spatial resolution depends on the quality of the electron optics.
- Quantitative analysis available on the base of NEXAFS and chemical shift Mounting in any position, with optional retracting device.
- Very large field of view using a of 40 mm diameter fiber optic detector
- Magnification up to ×8000.

However

- Needs ultra high vacuum chamber.
- Does not accept wet samples, no solvent.
- Does not work if sample charges.
- Flat sample needed (< 20-30 nm rough).

References

[1] B. Gilbert, R. Andres, P. Perfetti et al. Charging phenomena in PEEM imaging and spectroscopy. *Ultramicroscopy*, 2000, 83: 129-139.

[2] R. Fink, M.R. Weiss, E. Umbach et al. Smart: a planned ultrahigh-resolution

spectromicroscope for BESSY II. *Journal of Electron Spectroscopy and Related Phenomena,* 1997, 84: 231-250.

[3] H. A. Padmore. Soft X-ray optics for spectromicroscopy at the Advanced Light Source. *American Institute of Physics.* 1997, 389: 193-207.

[4] S. Anders, T. Stammler et al. Investigation of slider surfaces after wear using photoemission electron microscopy. *Journal of Vacuum Science Technology, A.* 1999,17(5): 2731-2735.

[5] S. Anders, A. Scholl et al. Photoemission electron microscopy for the study of ferromagnetic and antiferromagnetic materials. *American Institute of Physics*. 2000, 521: 7-12.

[6] U. Kleineberg, D. Menke et al. Photoemission microscopy with microspot-XPS by use of undulator radiation and a high-throughput multiplayer monochromator at BESSY . *Journal of Electron Spectroscopy and Related Phenomena*. 1999, 101-103: 931-936.

[7] G.H. Fecher, Y.Hwu, W. Swiech, Chemical microimaging and microspectroscopy of surfaces with a photoemission microscope. *Surface Science*. 1997,377-379:1106-1111.

[8] W. Swiech, G.H. Fecher, M. Huth et al. characterization of structured thin films made from complex materials by photoabsorption spectromicroscopy. *Applied Physics*. *A* 1998, 67: 447-454.

[9] G.H. Fecher, Y. Hwu, Y. D. Yao et al. Photoabsorption and MXCD in photoemission microscopy for characterization of advanced materials. . *Journal of Electron Spectroscopy and Related Phenomena.* 1999, 101-103: 937-942.

[10] M. Zharnikov, M. Neuber, M. Grunze, Novel contrast mechanisms in photoelectron microscopy. *Journal of Electron Spectroscopy and Related Phenomena*. 1999, 98-99: 25-40.

[11] J. Stohr, H. A. Padmore, S. Anders et al. Principles of X-ray magnetic dichroism spectromicroscopy. *Surface Review and Letter*. 1998, 5(6): 1297-1308.

[12] T. Stammler, S. Anders et al. PEEM2 user manual of ALS.

[13] J. Almeida, C. Coluzza et al. Photoemission electron microscopy studies of

Pt/GaP(001) buried interfaces. *Journal of Applied Physics*. 1996, 80(3): 1460-1464.

[14] P. Hoffmann, R. P. Mikalo, D. Schmeiber, A spectro-microscopic approach for spatially resolved characterization of semiconductor structures in PEEM. Solid-State Electronics. 2000, 44: 837-843.

[15] S. Anders, T. Stammler et al. X-ray photoemission electron microscopy for the study of semiconductor materials. American Institute of Physics. 1998, 449:873-877.

[16] J. Bansmann, V. Senz et al. Ion islands and dots on W(110) studied with polarized synchrotron radiation. *Journal of Electron Spectroscopy and Related Phenomena*. 2000, 106: 221-232.

[17] A. Schaak, R, Imbihl, Triangular-shaped reaction fronts in a catalytic surface reaction. *Chemical Physics Letter*. 1998, 283: 386-390.

[18] A. Schaak, B. Nieuwenhuys and R. Imbihl, Anisotropic chemical waves on a stepped surface: the NO + H_2 and O_2 + H_2 reaction on Rh(533). *Surface Science*. 1999, 441: 33-44.

[19] G. D. Stasio, B. Gilbert, et al. Frontiers of x-ray spectromicroscopy in biology and medicine: Gadolinium in brain cancer. *American Institute of Physics.* 2000, 506: 577-584.

[20] O. Schmidt, Ch. Ziethen et al. Chemical microanalysis by selected-area ESCA using an electron energy filter in a photoemission microscopy . *Journal of Electron Spectroscopy and Related Phenomena*. 1998, 88-91: 1009-1014.

[21] N, Smith. Science with soft x-rays. Physics Today Online. 2001, 5(1): 1-6.